REGENERATIVE AMPLIFICATION FOR A HARD X-RAY FREE-ELECTRON LASER

G. Marcus, Y. Ding, Y. Feng, A. Halavanau, Z. Huang, J. Krzywinski, J. MacArthur, R. Margraf,
T. Raubenheimer, D. Zhu, SLAC National Accelerator Laboratory, Menlo Park, CA 94025, USA
V. Fiadonu, Santa Clara University, Santa Clara, CA 95053, USA

Abstract

An X-ray regenerative amplifier FEL (XRAFEL) utilizes an X-ray crystal cavity to provide optical feedback to the entrance of a high-gain undulator. An XRAFEL system leverages gain-guiding in the undulator to reduce the cavity alignment tolerances and targets the production of longitudinally coherent and high peak power and brightness X-ray pulses that could significantly enhance the performance of a standard single-pass SASE amplifier. The successful implementation of an X-ray cavity in the XRAFEL scheme requires the demonstration of X-ray optical components that can either satisfy large output coupling constraints or passively output a large fraction of the amplified coherent radiation. Here, we present new schemes to either actively Q-switch a diamond Bragg crystal through lattice constant manipulation or passively output couple a large fraction of the stored cavity radiation through controlled FEL microbunch rotation. A beamline design study, cavity stability analysis, and optimization will be presented illustrating the performance of potential XRAFEL configurations at LCLS-II/-HE using high-fidelity simulations.

INTRODUCTION

The production of longitudinally coherent radiation from single-pass self-amplified spontaneous emission (SASE) FEL amplifiers has been the subject of continued interest. Cavity-based X-ray FELs (CBXFELs) [1] such as the X-ray free-electron laser oscillator (XFELO) [2] and the X-ray regenerative amplifier free-electron laser (XRAFEL) [3, 4] have seen renewed interest as a means of producing and preserving longitudinally coherent hard X-ray (HXR) FEL pulses. While the XFELO and XRAFEL schemes share a common infrastructure (a high-brightness, high repetition rate electron beam, an undulator, and an X-ray cavity) they target very different but complementary FEL performance characteristics (see, for example, [1] and references therein). The XFELO relies on a low-loss cavity supporting a low-gain FEL while the XRAFEL leverages a high-gain FEL interaction. Consequently, the requirements on the cavity for a XRAFEL are relatively relaxed. The science that is enhanced and/or enabled by these two concepts are therefore very different. Here, we focus on the practical elements and performance characteristics of an XRAFEL implementation of a CBXFEL at the LCLS-II facility.

The LCLS-II [5, 6] and the LCLS-II-HE upgrade [7, 8] will be capable of delivering high-brightness electron beams to the HXR undulator at repetition rates as high as ~ 1 MHz, making realistic X-ray cavity geometries and footprints fea-

sible. Significant cavity component development and evaluation has been undertaken by the team at Argonne National Lab in the context of the XFELO. They have shown that high quality diamond Bragg crystals have record-high reflectivities [9], ultra-low thermal expansion and high thermal diffusivity [10], and high mechanical and radiation hardness [11]. These properties make diamond an excellent candidate for the XRAFEL.

The flexibility of the high-gain XRAFEL system, however, allows for the investigation of strongly tapered undulators for high conversion efficiency of electrical to optical power. Efficient undulator tapering relies on stable, high power, and longitudinally coherent seed pulses [12, 13], which a RAFEL would excel at delivering. In this regard, diamond optics present a challenge because of their ultra-high reflectivities, making it difficult to extract a large fraction of the stored X-ray pusle energy. Here, we briefly present two methods that may be used to output couple a significant fraction of the stored cavity X-ray power. One method, cavity Q-switching, relies on a manipulation of the cavity optics while the second method, microbunch rotation and off-axis lasing, manipulates the gain medium itself (the electron bunch). We also explore the consequence of the Q-switching concept on the design of the cavity and the performance of the scheme.

RADIATION OUTPUT COUPLING METHODS

Various output coupling methods have been explored within the context of an XRAFEL implementation at the LCLS-II facility. These include both active and passive methods that require manipulation of either the cavity optical components or the gain medium iteslf. We briefly present two concepts below.

Transient Thermal Expansion of Diamond Lattice Constant

Transient thermal expansion of the diamond lattice constant can be achieved through short-pulsed optical laser excitation. The lattice spacing, therefore, can be manipulated to satisfy or not satisfy the Bragg reflection condition on demand - the cavity can be actively 'Q-switched'. The thermal transport time scale of absorbed energy out of the primary absorbed region on the crystal is 10's of ns due to the high thermal conductivity of diamond, which is sufficiently short compared to a typical roundtrip time in the cavity ($\sim 1\mu s$ for LCLS-II). Since all of the cavity power is dumped through this process, the effective repetition rate of the XRAFEL is lowered from ~ 1 MHz to $\sim 10-50$ kHz, and depends on

the number of passes needed for the XRAFEL to reach a steady-state saturated condition from start up. However, it opens the possibility of producing and dumping high *peak* power and fully coherent FEL pulses.

Initial simulations including a time-dependent heat analysis of the diamond crystal surface has shown that it is extremely difficult to get a uniform temperature profile to a depth of an extinction length ($\sim 5 \mu m$ for the parameters studied here). A novel technique has been explored to enable a more uniform temperature profile. This technique leverages a boron doped buried layer under the surface of the diamond to increase the absorption of light in the infrared part of the spectrum. A program has been initiated to experimentally investigate this technique. More detail can be found in [14].

Off-axis Lasing Through Controlled Microbunch Rotation

The microbunches in an electron beam can be rotated in a defocusing quadrupole or in a quadrupole triplet, which can then radiate off-axis in a re-pointed undulator [15, 16]. This scheme opens the possibility of passively output coupling radiation from an XRAFEL cavity through gain medium manipulation. The off-axis radiation can either bypass the post-undulator diamond crystal with a strong enough kick or can possibly fall outside the diamond rocking curve and therefore be transmitted. The on-axis radiation can be recirculated and used to seed the next electron bunch. In this way, the nominal ~ 1 MHz repetition rate of the LCLS-II can be maintained while the XRAFEL produces high *average* power .

The quadrupole triplet scheme was tested at LCLS where HXR microbunch rotation greater than 5 microradian at a 9.5 keV photon energy was experimentally demonstrated. The quadrupoles of the LCLS undulator FODO lattice were used to perform the microbunch rotation (see Figure 1c). During this shift, roughly 850 μJ pulse energy was split evenly between two spots (see Figure 1a). Various rotation angles were also explored (see Figure 1b). More details on this scheme can be found in [17].

XRAFEL CAVITY DESIGN

We begin with the assumption that the X-ray cavity will adopt, as an initial implementation, a rectangular geometry (see Figure 2a). Two compound refractive lenses provide focusing, and when symmetrically placed within the cavity, provide radiation waists at the locations marked $w1$ and $w2$. This particular geometry is being explored because it fits into the LCLS undulator hall, works for both the XFELO and XRAFEL schemes, is being studied as part of the CBXFEL project [1], and can be upgraded to a tunable geometry [18]. The equivalent unfolded optical lattice of the cavity is shown in Figure 2b. Gaussian beam ABCD optics provides a suitable framework with which to analyze the system [19]. Within this framework, one can find the complex Gaussian 'eigen-q' of the system, which defines the self-reproducing mode that is self-consistent upon round

(a)

(b)

(c)
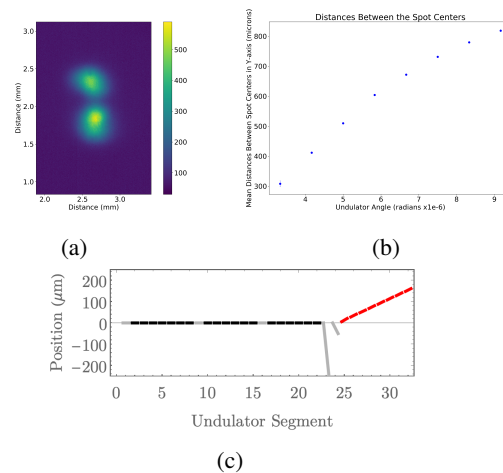
Figure 1: (a) Two transverse spots with equal energy on the post-undulator direct imager. (b) Spot separation on the direct imager as a function of the undulator pointing. (c) LCLS undulator configuration for microbunch rotation at a particular angle.

(a)

(b)
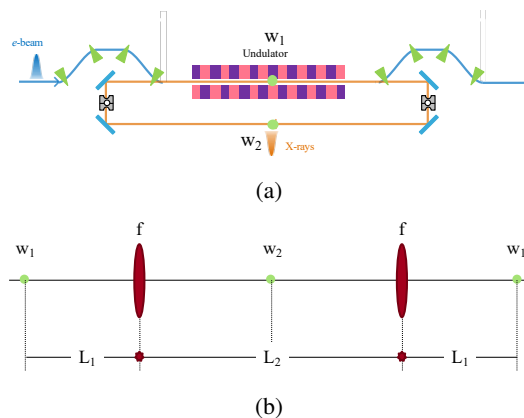
Figure 2: (a) Mockup of the rectangular cavity. (b) Unfolded equivalent optical lattice.

trip propagation:

$$q_o = \frac{A q_i + B}{C q_i + D} = q_i. \qquad (1)$$

Here, q_i and q_o are the initial and propagated complex beam parameters, respectively, and depend on the ABCD matrix elements of the optical system. This equation has two solutions:

$$\frac{1}{q_{a,b}} = \frac{D - A}{2B} \mp \frac{1}{B} \sqrt{m^2 - 1}, \qquad (2)$$

where $m = (A + D)/2$. The m parameter determines the stability of the cavity both in the context of stable or unstable periodic focusing systems and in terms of the self-consistent eigensolutions, $q_{a,b}$ being stable against small perturbations. A stable cavity will have $-1 < m < 1$ while the period of oscillation (either geometrically or perturbatively) is given by $\theta = \cos^{-1}(m)$.

The strategy for choosing $L1, L2$ and f is as follows. First, the $w1$ that is equivalent to the guided mode solution in the high gain FEL is solved for under the constraints that $2L_1 + L_2 = L_{cav}$ for a stable cavity and that all matrix elements (A, B, C, D) are real. One advantage of the high gain XRAFEL is that it can tolerate significant radiation losses in the cavity. It is possible for the radiation to make multiple round trips in the cavity before interacting with a following fresh electron beam. Depending on the electron beam repetition rate and the total cavity length (L_{cav}), L_2 can be chosen such that the the period of perturbation oscillation, θ, matches the period of radiation-beam interaction. Another advantage of chosing $w1$ to be the guided mode solution is that the radiation at the entrance of the undulator after propagating through the cavity is larger than this solution and is slightly converging. The larger field size makes the XRAFEL slightly less susceptible to lateral and angular displacements (errors) and the seed field intensity nominally increases as the radiation approaches the waist. This is advantageous for strong undulator tapering. Finally, the high-gain XRAFEL system can gain guide laterally or angularly displaced seed radiation back to the undulator axis and can significantly correct mirror angular displacement errors.

CAVITY STABILITY ANALYSIS

After performing the above design optimization, a root sum square (RSS) statistical tolerancing analysis, similar to what has been performed in [1], can be performed for the XRAFEL given the cavity parameters $L1, L2, f$. Here, it is assumed that the cavity wraps the entire undulator, has a total cavity length $L_{cav} \sim 323$ m, and supports three round trips of the X-ray pulse before interacting with a following fresh electron bunch (assuming 100 pC charge electron bunch parameters for an LCLS-II-HE scenario, the parameters of which can be found in [7]). These initial estimates project a mirror angular error tolerance of $\sigma_m \sim 70$ nrad.

Gain guiding, however, is not currently captured in the analytical tolerancing analysis. Here, we present preliminary results of time-independent GENESIS [20] simulations for the case presented above for the production of 9.8 keV photons. The electron bunch length for this scenario is similar to the Fourier-limited pulse length associated with diamond (400) crystal plane reflectivity making the single-frequency simulations a reasonable approximation. Figure 3 shows the results of $\sim$ 150 simulations where the angular errors of the four cavity mirrors were assumed to be independent and normally distributed with RMS errors of $\sigma_m = 0.35 \mu$rad (top row) and $\sigma_m = 0.5 \mu$rad (bottom row). Each simulation included modeling the diamond mirror net efficiencies assuming the output coupling crystal was Q-switched using the technique described above and propragating the radiation fields through the cavity using standard Fourier optics techniques. The 3-pass roundtrip efficiency in this case was $\sim 5\%$. Without any mirror errors, the saturated power of the radiation after the 30th interaction with the electron beam is ~ 4 GW. Figures 3b and 3d indicate that roughly 4% and
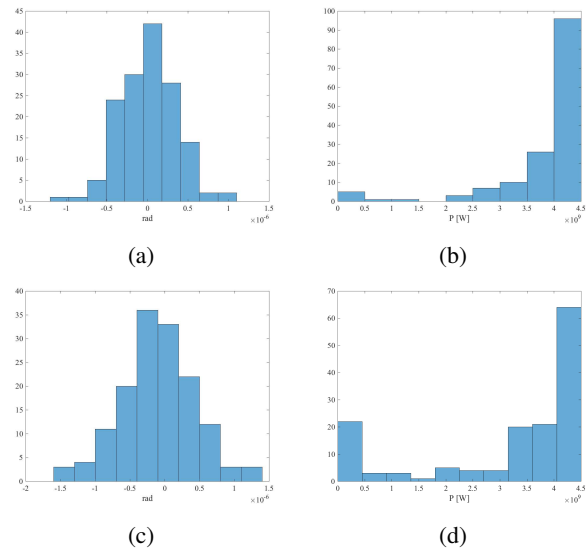
Figure 3: (a) Histogram of M1 errors for $\sigma_m = 0.35 \mu$rad. (b) Histogram of final power after 30 interactions of the radiation with the electron beam in the cavity for $\sigma_m = 0.35 \mu$rad. (c) Histogram of M1 errors for $\sigma_m = 0.5 \mu$rad. (b) Histogram of final power after 30 interactions of the radiation with the electron beam in the cavity for $\sigma_m = 0.5 \mu$rad.

25% of the final power levels do not reach an appreciable level of 1 GW. Note that a $\sigma_m = 0.35 \mu$rad mirror error is 5 times the analytic estimate. A further reduction in the mirror error in simulation will results in less low-power shots.

DISCUSSION

An XRAFEL implementation at LCLS-II/-HE offers a compelling pathway for the production fully coherent high average and peak power hard X-ray FEL pulses. A number of options exist for output coupling a large fraction of the stored cavity power, only two of which were presented here. These schemes include both active and passive methods and rely on both cavity optics as well as gain medium manipulations. Gain guiding in the high-gain FEL process relaxes the alignment and stability requirements of the cavity optomechanical systems.

ACKNOWLEDGEMENTS

REFERENCES

[1] G. Marcus *et al.*, "Cavity-based free-electron laser research and development: a joint Argonne national laboratory and SLAC national laboratory collaboration", presented at FEL'19, Hamburg, 2019, paper TUD04, this conference.

[2] K.-J. Kim, Y. Shvyd'ko, and Sven Reiche, "A proposal for an x-ray free-electron laser oscillator with an energy-recovery linac" *Phys. Rev. Lett.* vol. 100, pp. 244802, 2008, `doi:10.1103/PhysRevLett.100.244802`

[3] Z. Huang and R.D. Ruth, "Fully coherent x-ray pulses from a regenerative-amplifier free-electron laser", *Phys. Rev. Lett.* vol. 96, pp. 144801, 2006, `doi:10.1103/PhysRevLett.96.144801`

[4] G. Marcus *et al.*, "X-ray regenerative amplifier free-electron laser concepts for LCLS-II", in *Proc. 38th Int. Free-Electron Laser Conf.*, New Mexico, 2017, `doi:10.18429/JACoW-FEL2017-MOP061`

[5] T.O. Raubenheimer, ed., "LCLS-II final design report", SLAC, Menlo Park, CA, LCLSII-1.1-DR-0251-R0, 2015.

[6] T.O. Raubenheimer, "Technical challenges of the LCLS-II CW x-ray FEL", in *Proc. 6th Int. Particle Accelerator Conf.*, Virginia, USA, 2015, `doi:10.18429/JACoW-IPAC2015-WEYC1`

[7] T.O. Raubenheimer, ed., "LCLS-II-HE conceptual design report", SLAC, Menlo Park, CA, LCLSIIHE-1.1-DR-0001-R0, 2018.

[8] T.O Raubenheimer, "The LCLS-II-HE, a high energy upgrade of the LCLS-II", 60th *ICFA Advanced Beam Dynamics Workshop on Future Light Sources*, Shanghai, China, 2018, `doi:10.18429/JACoW-FLS2018-MOP1WA02`

[9] Yuri Shvyd'ko *et al.*, "Near-100% Bragg reflectivity of x-rays", *Nat. Phot.* 5, pp. 539, 2011, `doi:10.1038/nphoton.2011.197`

[10] S. Stoupin, Y. Shvyd'ko, "Thermal expansion of diamond at low temperatures", *Phys. Rev. Lett.* vol. 104, pp. 085901, 2010, `doi:10.1103/PhysRevLett.104.085901`

[11] T. Kolodziej *et al.*, "High Bragg reflectivity of diamond crystals exposed to multi-kW mm^2 x-ray beams", *J. of Synch. Rad.*, vol. 25, pp. 1022, 2018, `doi:10.1107/S1600577518007695`

[12] C. Emma *et al.*, "High efficiency, multiterawatt x-ray free electron lasers", *Phys. Rev. Accel. and Beams*, vol. 19, pp. 020705, 2016, `doi:10.1103/PhysRevAccelBeams.19.020705`

[13] J. Duris, A Murokh and P. Musumeci, "Tapering enhanced stimulated superradiant amplification", *New J. of Phys.*, vol. 17, pp. 063036 2015, `doi:10.1103/PhysRevAccelBeams.21.080705`

[14] J. Krzywinski *et al.*, "Q-Switching of X-Ray Optical Cavities With a Boron Doped Buried Layer Under the Surface of a Diamond Crystal", presented at FEL'19, Hamburg, 2019, paper TUP033, this conference.

[15] J. MacArthur *et al.*, "Microbunch rotation and coherent undulator radiation from a kicked electron beam", *Phys. Rev. X*, vol. 8, pp. 041036, 2018, `doi:10.1103/PhysRevX.8.041036`

[16] J. MacArthur *et al.*, "Microbunch rotation and coherent undulator radiation from a kicked electron beam", presented at FEL'19, Hamburg, 2019, paper MOD02, this conference.

[17] R. Margraf *et al.*, "Microbunch rotation for hard x-ray beam multiplexing", presented at FEL'19, Hamburg, 2019, paper THP036, this conference.

[18] Yuri Shvyd'ko, "Feasibility of x-ray cavities for free electron laser oscillators", *ICFA Beam Dynamics Newsletter*, No. 60, 2013.

[19] A. Siegman, *Lasers*, University Science Books, 1986.

[20] S. Reiche, "GENESIS 1.3: a fully 3D time-dependent FEL simulation code", *Nucl. Instr. Meth. Phys. Res. Sec. A*, vol. 429, pp. 243, 1999, `doi:10.1016/S0168-9002(99)00114-X`